Dev Genes Evol (2014) 224:235–244
DOI 10.1007/s00427-014-0480-1

ORIGINAL ARTICLE

Dynamic expression of a *Hydra* FGF at boundaries and termini

Ellen Lange · Stephanie Bertrand · Oliver Holz · Nicole Rebscher · Monika Hassel

Received: 11 June 2014 / Accepted: 17 September 2014 / Published online: 14 October 2014

Abstract Guidance of cells and tissue sheets is an essential function in developing and differentiating animal tissues. In *Hydra*, where cells and tissue move dynamically due to constant cell proliferation towards the termini or into lateral, vegetative buds, factors essential for guidance are still unknown. Good candidates to take over this function are fibroblast growth factors (FGFs). We present the phylogeny of several *Hydra* FGFs and analysis of their expression patterns. One of the FGFs is expressed in all terminal regions targeted by tissue movement and at boundaries crossed by moving tissue and cells with an expression pattern slightly differing in two *Hydra* strains. A model addressing an involvement of this FGF in cell movement and morphogenesis is proposed: *Hydra FGFf*-expressing cells might serve as sources to attract tissue and cells towards the termini of the body column and across morphological boundaries. Moreover, a function in morphogenesis and/or differentiation of cells and tissue is suggested.

Keywords Cell and tissue movement · Guidance cue · Evolution · Differentiation · Morphogenesis

Communicated by Volker G. Hartenstein

Electronic supplementary material The online version of this article (doi:10.1007/s00427-014-0480-1) contains supplementary material, which is available to authorized users.

E. Lange · O. Holz · N. Rebscher · M. Hassel (✉)
Faculty of Biology, Morphology and Evolution of Invertebrates, Philipps-Universität Marburg, Karl-von-Frisch-Str. 8, 35032 Marburg, Germany
e-mail: hassel@biologie.uni-marburg.de

E. Lange
e-mail: ellen.lange@biologie.uni-marburg.de

O. Holz
e-mail: holzo@students.uni-Marburg.de

N. Rebscher
e-mail: rebscher@biologie.uni-marburg.de

S. Bertrand
Sorbonne Universités, UPMC Univ Paris 06, Paris, France
e-mail: stephanie.bertrand@obs-banyuls.fr

S. Bertrand
CNRS, UMR 7232, BIOM, Observatoire Océanologique, 66650 Banyuls-sur-Mer, France

Introduction

Fibroblast growth factors (FGFs) and their receptors (FGFRs) originated early in animal evolution and were present already in the common eumetazoan ancestor of Cnidaria and Bilateria (Bertrand et al. 2014; Rebscher et al. 2009). In triploblastic animals, they control key functions like cell and tissue movement (Kadam et al. 2009; Klingseisen et al. 2009), branching morphogenesis and boundary formation (Affolter et al. 2009). In mammals, FGF ligands constitute a superfamily of 22 multifunctional growth factors, which can be classified into seven subfamilies (Itoh and Ornitz 2011). In fish, more FGFs exist, e.g. FGF24, which also belong to the seven subfamilies (Jovelin et al. 2010). Most FGFs act as paracrine growth factors and are subdivided into FGF1/2, FGF4/5/6, FGF3/7/10/22, FGF8/17/18/24 and FGF9/16/20 subfamilies. FGF15/19/21/23 subfamily members (FGF 15 and 19 are mouse/human orthologs) act as endocrine hormone-like molecules controlling physiology and homeostasis whereas FGF11/12/13/14 are intracellular factors which have functions in neural development and influence the activity of voltage-gated sodium channels (reviewed in Itoh and Ornitz (2011)). This high complexity of ligands compared to non-vertebrate metazoans is, in part, the result of the two whole genome duplications that took place at the origin of the vertebrate lineage (Dehal and Boore 2005).

In protostomes as well as in the deuterostomes *Saccoglossus kowalevskii* and *Branchiostoma floridae*, members of the paracrine FGF1/2 and FGF8/17/18/24 subfamilies have been described or predicted (Bertrand et al. 2014; Oulion et al. 2012), while the urochordate *Ciona intestinalis* possesses seven FGFs, five of which were assigned to FGF3/7/10/22, FGF4/5/6, FGF8/17/18/24, FGF9/16/20 and FGF11/12/13/14 subfamilies (Satou et al. 2002). In the fly *Drosophila melanogaster* and in the nematode *Caenorhabditis elegans*, FGF ligands of the FGF8/17/18/24 subfamily (Pyramus and Thisbe in *Drosophila* and Egl-15 in nematode) are indispensable for normal migration of mesodermal cells and tissue sheets, as well as in the fly for muscle and heart development (Huang and Stern 2005; Kadam et al. 2009; Muha and Muller 2013). The FGF ligand Branchless found in arthropods was shown to control morphogenesis of tracheal tubules and neurogenesis in *Drosophila* (reviewed in Muha and Muller (2013)). Concerning Cnidaria, up to 14 FGF genes were predicted in the sea anemone *Nematostella vectensis* (Matus et al. 2007), and it has been shown that two of them and two FGFRs antagonistically control the formation of the embryonic apical organ (Rentzsch et al. 2008). In the freshwater polyp *Hydra*, expression of a first FGF was described recently (Krishnapati and Ghaskadbi 2013). FGFs have not yet been investigated functionally, but since Kringelchen, one of the two *Hydra* FGFRs (Rudolf et al. 2012), is indispensable for morphogenesis and detachment of vegetative buds (Sudhop et al. 2004) essential functions in tissue dynamics are likely.

In this study, we searched expressed sequence tag (EST) and genomic databases for *Hydra* FGFs and established a phylogenetic tree based on the predicted protein sequences. To obtain first clues as to potential functions, the expression patterns of five FGFs was analysed. We present evidence for the early presence of four FGFs and a highly dynamic expression pattern of *FGFf* at boundaries and in all terminal structures. Potential functions in chemoattraction of cells and morphogenesis of the body structures are discussed.

Material and methods

Search for Hydra FGF sequences

To identify *Hydra* FGF sequences, we screened the NCBI, JGI hydrazome/metazome databases, Compagen (http://www.compagen.org/), T-CDS: transcript models (contigs) derived from assembled ESTs (Sanger, 454, etc.) (Hemmrich et al. 2007; Hemmrich and Bosch 2008) and a recent RNASeq project (Wenger and Galliot 2013) for annotated FGFs and using the core region sequence of known vertebrate FGFs (Fig. S1). The data were then expanded in a new and complete alignment.

Phylogenetic analysis

FGF domain amino acid sequences were retrieved for vertebrates, *C. intestinalis*, *Branchiostoma lanceolatum*, *Acropora digitifera*, *Hydra magnipapillata*, *Hydra vulgaris*, *N. vectensis*, and several protostome species. BLASTP or TBLASTN were used at different databases with sequences of the FGF domain from the different FGF subfamilies as queries. Databases and accession numbers are indicated in Figs. S2 and S3. FGF19/21/23 sequences from vertebrates were not included because the FGF domain is incomplete. FGF domain amino acid sequences were aligned using hmmalign implemented in HMMER 3.0 (Eddy 2008) based on the FGF profile HMM (Pfam PF00167) on the Mobyle portal (Neron et al. 2009). The alignment was then manually reviewed in SeaView (Gouy et al. 2010). Final alignment used for phylogenetic analyses is given in supplementary Fig. S4. Bayesian inference (BI) trees were inferred using MrBayes 3.1.2 (Ronquist F et al. 2012), with the model recommended by ProtTest 3 (Abascal et al. 2005) under the Akaike information criterion (WAG+Γ), at the CIPRES Science Gateway V. 3.1. Two independent runs were performed, each with four chains and one million generations. A burn-in of 25 % was used and a 50 majority rule consensus tree was calculated for the remaining trees. Maximum likelihood (ML) analyses were performed using RAxML version 8.0.9 (ref is: A. Stamatakis: "RAxML Version 8: A tool for Phylogenetic Analysis and Post-Analysis of Large Phylogenies". In *Bioinformatics*, 2014, open access) with the same model as for BI and the rapid bootstrapping algorithm. The phylogenetic tree obtained using ML has a topology consistent with the topology obtained by BI but shows low branch supports (supplementary Fig. S5).

Animal care

Hydra vulgaris AEP was kept in a medium consisting of $CaCl_2$, $MgSO_4$, $NaHCO_3$ and K_2CO_3 in MilliQ H_2O, pH 7.4 at 18 °C. To synchronize bud development, polyps were fed five times a week and starved for 2 days (Sudhop et al. 2004).

Regeneration of Hydra polyps

Regeneration for analysis of FGFf expression was induced 24 h after feeding by bisection of the body column. Ten about equally sized budless polyps were bisected. Head and foot fragments were stored separately in 6-well plates each and evaluated at the given time points.

Cloning of *Hydra* FGF cDNAs

Poly(A)+ RNA was prepared from Hydra using the QuickPrep Micro Kit, Amersham and transcribed into complementary

DNA (cDNA) using RevertAid^{TM} Premium First-strand cDNA Synthesis Kit. Partial sequences of *Hydra* FGFs were amplified from this cDNA by PCR using the following primer pairs (Fig. S3):

FGFa (forward: HA_FGFa_fw: CACATACTGAAACT TTTTAGTCCC, reverse: HA_FGFa_rv: ATAAGCAT CATCAAACAGTTCCC),
FGFc (forward: HA_FGFc_fw: GCAAAAGGAATGGA GCGCAG, reverse: HA_FGFc_rv: ACTCGAGTAACT ACTGTCCTAG),
FGFe (forward: HA_FGFe_fw: TATTACGGAGATTC ACGATGTTG, reverse: HA_FGFe_rv: TTGGAGCA CTGGACGTGTTAG) and
FGFf (forward: HA_FGFf_fw: CGCTTGCAGAACCG ACTCATG, reverse: HA_FGFf_rv: ACTCATCGTTGG AAGCCACATG).

The PCR fragments were cloned into pGEM-T Easy, sequenced by SeqLab and used for RNA probe synthesis. Whole sequences will be annotated and submitted to GenBank.

Semi-quantitative RT-PCR for Hydra ***FGFf*** and ***EF1α***

Thirty milligram *H. v*ulgaris *AEP* and *H. magnipapillata*, each consisting of 30 stage 9 and 18 stages 5–7 specimen, were homogenized rapidly in 500 μl TRI Reagent (Ambion) with an RNAse-free mini-pistil and incubated 5 min at room temperature. The homogenate was cleared by centrifugation (5 min 13,000 rpm) and the supernatants were transferred using a 1-ml syringe with a 20-gauge needle to Direct-zol spin columns (Zymo). Total RNA purification was carried out according to the manufacturer's instructions including an on-column digestion step with DNase I. First-strand cDNA synthesis with oligo dT primers was carried out from 1 μg total RNA using the RevertAid H-Minus first-strand cDNA synthesis kit (Thermo Scientific). PCR primers (Tm 58–60 °C) were: EF1α fw 5 -AAAGCTGAACGTGAAAGAGGT-3 , EF1α rev 5 -ACCA GTCTCAACACGACCAA-3 , FGFf fw 5 -CATAACCACA TCCGAAAACCCT-3 and FGFf rev5 -GTGCCACTCATC GTTGGAAG-3 . PCR reactions were set up as follows: H_2O 12.9 μl, 10× PCR Buffer B (Axon) 2 μl, 25 mM $MgCl_2$ solution 1.5 μl, 10 mM dNTP mix 0.4 μl, 10 μM primer fw 1 μl, 10 μM primer rev 1 μl, cDNA 1 μl (pure for FGFf or diluted 1:5 in H_2O for EF1 α), 5 U/μl Taq polymerase (Axon) 0.2 μl. PCR conditions were: 2 min 95 °C, 1 min 95 °C, 1 min 54 °C, 1 min 72 °C, 29×, 10 min 72 °C. For each PCR reaction, 10 μl were separated on a 0.8 % agarose gel.

In situ hybridization

Whole mount in situ hybridization was performed as described previously (Sudhop et al. 2004) with the exception that the proteinase K digest was prolonged from 10 to 15 min for *H. vulgaris AEP*. Digoxigenin-labelled RNA probes were synthesized using the Roche Dig-labelling system. Integrity and size of the RNA probes was verified by northern blotting and about 300 ng of the synthetic RNA were used for the in situ hybridization. Bud stages were selected and assigned according to (Otto and Campbell 1977).

Results and discussion

FGFs may substantially vary in size, but all of them contain a characteristic core region. By searching genomic and EST databases using this core sequence (Fig. S1), we identified already annotated and new FGFs from various *Hydra* strains (Fig. 1 and Supplement S2, S3). We numbered the *Hydra* FGFs alphabetically whenever a clear assignment was not possible.

Phylogeny of *Hydra* FGFs identifies members of the paracrine FGF subfamilies as well as of independent FGF families

In a phylogenetic tree rooted by the FGF8 group (Fig. 1) including *Hydra* as well as other cnidarian sequences, we recover with good support the known vertebrate subfamilies. Among cnidarian sequences, we found clear members of the FGF8/17/18/24 subfamily whereas some of the sequences seem to group with the FGF1/2 subfamily although with low support values. Both FGF subfamilies comprise paracrine FGF ligands, which are secreted in the interstitium and thus active over longer distances (Itoh and Ornitz 2011). A third group of cnidarian FGF sequences is recovered and is placed with the intracellular FGF11/12/13/14 and the paracrine FGF9/16/20 subfamilies although orthology assignment is not clear from our data. These results support the hypothesis that three subfamilies of FGFs were present in the ancestor of eumetazoans among which at least FGF1/2 and FGF8/17/18/24 (Oulion et al. 2012).

Our phylogenetic analysis of the predicted FGF sequences also shows that cnidarian-specific duplications of FGF genes probably occurred several times which amplified the number of FGFs resulting in a highly diversified FGF gene set in each lineage. Indeed, we found several members in the three cnidarian FGF groups. However, the precise relationships between the different cnidarian sequences among each group is not resolved, leaving open the question of independent duplications in each cnidarian lineage or duplications in the ancestor of cnidarians. Within the FGF8/17/18/24 group, four *Nematostella* sequences and three *Hydra* ESTs are positioned together with *HvAEP_FGFf* (*FGFf*). The latter FGF is placed

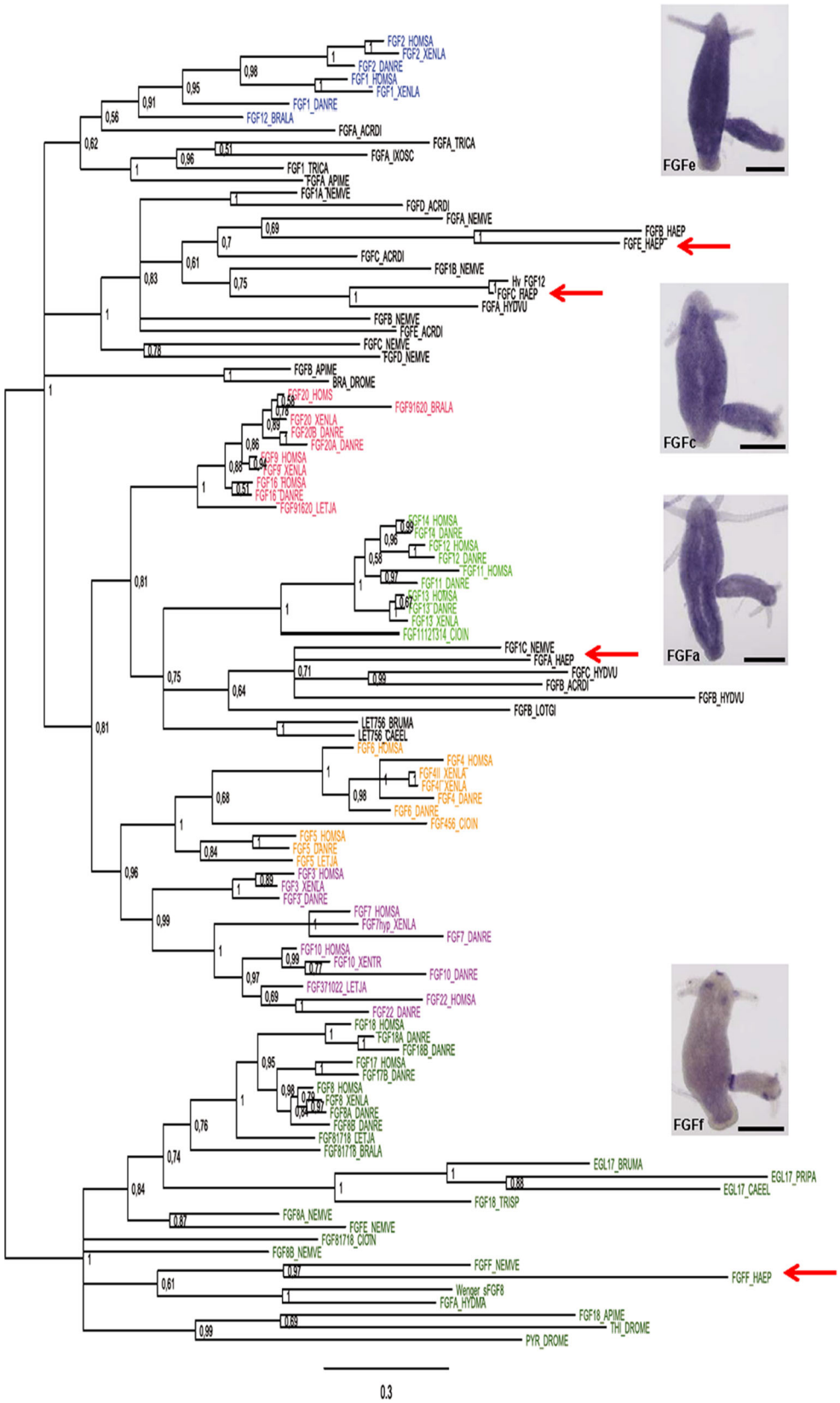

on a particularly long branch in the phylogenetic tree indicating a fast evolving gene. The FGFf sequence contains several insertions and deletions compared to other FGFs (Fig. 1b). Our initial idea that we had missed intron-exon boundaries

◀ **Fig. 1** Phylogenetic tree of FGFs using the FGF core sequence and expression pattern in *Hydra vulgaris Zürich* polyps. HOMSA *Homo sapiens*, XENLA *Xenopus laevis*, XENTR *Xenopus tropicalis*, DANRE *Danio rerio*, CIOIN *Ciona intestinalis*, NEMVE *Nematostella vectensis*, Hv *Hydra vulgaris Zürich*, HAEP *Hydra vulgaris AEP*, Wenger *Hydra vulgaris*, HYDVU *Hydra vulgaris*, HYDMA *Hydra magnipapillata*, LOTGI *Lottia gigantea*, TRICA *Tribolium castaneum*, IXOSC *Ixodes scapularis*, APIME *Apis melifera*, DROME *Drosophila melanogaster*, BRUMA *Brugia malayi*, TRISP *Trichinella spiralis*, PRIPA *Pristionchus pacificus*, CAEEL *Caenorhabditis elegans*, ACRDI *Acropora digitifera*, LETJA *Lethenteron japonicum*, BRALA *Branchiostoma lanceolatum*. The *insets* show the expression patterns of *Hydra* FGFs assigned to the respective FGF groups. *Scale bar*=100 μm

could not be confirmed, and so, we will have to wait for protein data to see what its properties are. For the moment, it is interesting to note that *FGFf* is expressed in a very dynamic pattern (see below).

Hydra FGFs are expressed differentially

Function of a gene in morphogenesis is often correlated to spatiotemporal changes in its expression profile. We therefore analyzed the expression patterns of five *H. vulgaris AEP* FGFs grouping in the different branches. The *FGFa*, *FGFc* and *FGFe* messenger RNAs (mRNAs) were detected almost ubiquitously in parent and bud with a reduced level of the mRNAs in the hypostome, i.e. the region between mouth opening and tentacle bases (Fig. 1). All three FGFs are expressed in the tentacle base endoderm, but not or only weakly in the tentacles. *FGFb* could not be detected by in situ hybridization, and since ESTs exist, it might either be expressed at very low levels or only under certain circumstances. This issue was not followed further.

FGFf, in contrast, shows a striking differential expression pattern: strong endodermal expression occurs in the tentacle tips, at the adult basal disc and a weak band is detectable right at the tentacle bases (Fig. 1 and details in Figs. 2 and 3). Moreover, *FGFf* is dynamically expressed during budding, when complete morphogenesis of a young polyp occurs (Fig. 2a–w). The ten bud stages (Otto and Campbell 1977) comprise an early tissue evagination phase (stages 1–3), an elongation phase of the bud (stages 4–7) and a detachment phase (stages 8–10). The earliest sign of *FGFf* expression was detected in a few endodermal cells of the evaginating bud tip (Fig. 2c, d and close-up in h, i). From stage 3 onwards, expression started in ectodermal cells, which completely covered the elongating bud tip in stage 4 (Fig. 2e, f, j, k). When the bud further elongated, a zone of weak expression became established from stage 5 onwards at the bud-parent boundary (Fig. 2l, m). The apical expression domain successively weakened and fragmented into first ectodermal (Fig. 2r–t) and later exclusively endodermal patches in the tentacle buds (Fig. 2o–q, u–w). Once the tentacles started to elongate, strong expression became restricted to the tentacle tip endoderm as seen in fully grown tentacles (Fig. 2q, w). In stages 8–10, a basal ring of *FGFf* expression in ecto- and endodermal cells correlated with the onset and termination of the detachment phase. Freshly detached buds showed the expression pattern of adult polyps with endodermal localization of the mRNA exclusively.

The highly dynamic expression pattern with switches between the two epithelial layers and regionalized, stage specific changes, indicates a gene subject to fine-tuned expression regulation (and thus probably essential functions) during morphogenesis. Similar switches during budding had been described previously already for the FGFR *kringelchen* (Sudhop et al. 2004).

Conserved *FGFf* expression pattern in *Hydra vulgaris Zürich*

Provided *H. vulgaris AEP FGFf* fulfils essential functions, its expression pattern (and functions) should be conserved across *Hydra* strains. In fact, the probe also detects the *FGFf* mRNA in *Hydra vulgaris Zürich*—interestingly with a generally stronger and unexpected intensity. This result was unexpected, because *Hydra vulgaris AEP* sequence is certainly not identical to *Hydra vulgaris Zürich* and about 10 % deviations are expected as deduced from other cDNA sequences (own observations). The different labelling intensities observed by ISH could not be corroborated by RT-PCR (Fig. S6) and might be due to permeability problems during in situ hybridization with *H. vulgaris AEP* despite the prolonged digestion with proteinase K. Besides strong expression in the endoderm of tentacle tips and basal disc (Fig. 3a), additional weak expression was detected throughout the whole-body column ectoderm and at all boundaries crossed by moving cells and tissue sheets. This applies to a ring of weak ectodermal expression right above the adult basal disc, which correlates with the zone where epithelial cells of the body column enter the basal disc and undergo terminal differentiation, and, it also applies to the boundaries between body column and protruding structures like tentacles or buds.

Moreover, early evaginating buds (Fig. 3a) are well detectable by an irregularly shaped patch of *FGFf*-expressing cells. Its position slightly apical to and at an angle of about 120 ° to the stage 8 bud on the right side of the parent (Fig. 3a) is a typical position for an emerging bud. The patchy expression pattern with interspersed cells expressing the gene strongly corresponds to that observed in the stage 3 bud of *H. vulgaris AEP* (Fig. 2d, i).

Comparison of *FGFf* expression between the two strains thus reveals that the expression domains are identical with the exception of the weak ectodermal expression right above the basal disc in *H. vulgaris Zürich* and the broader proximal belt

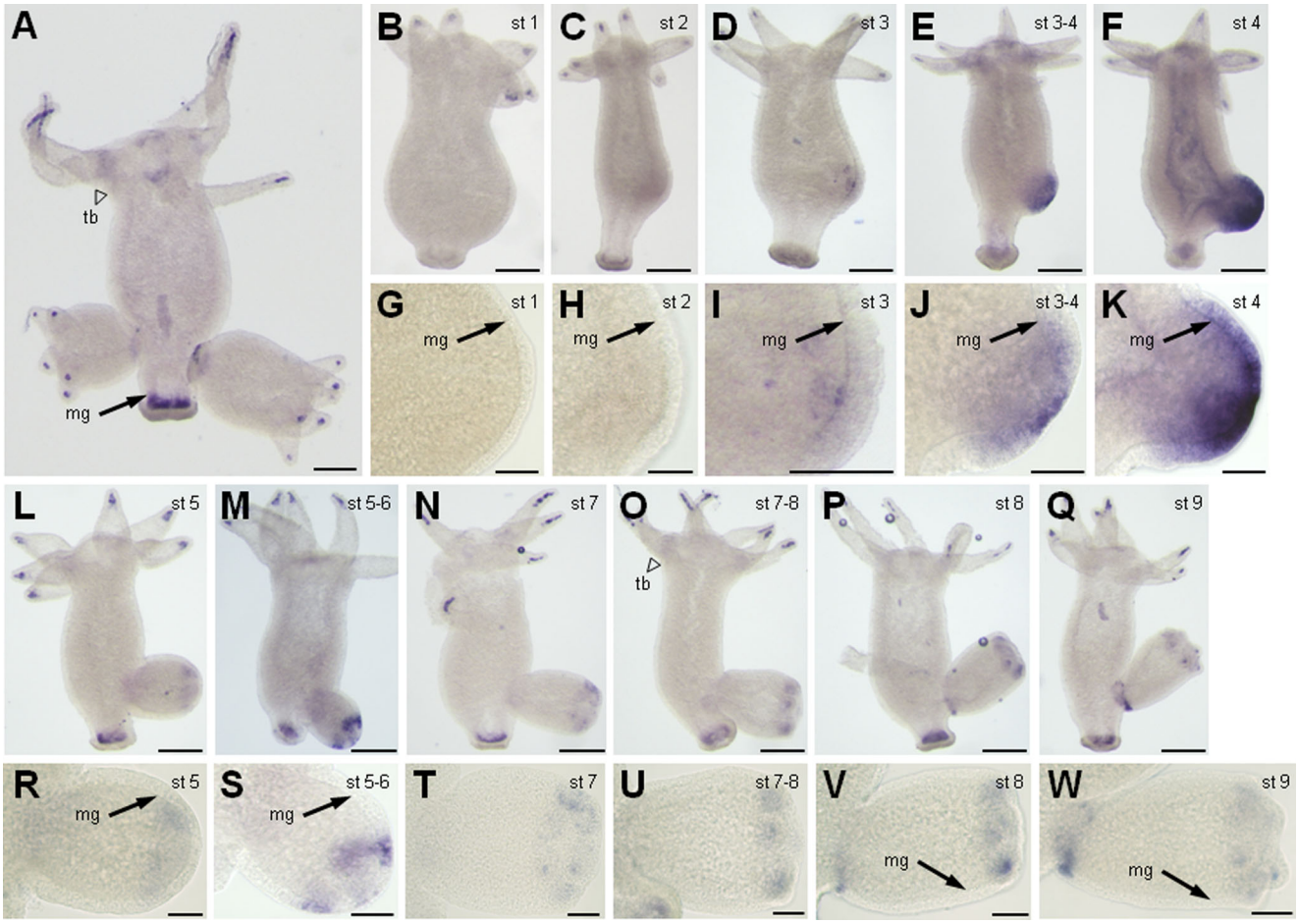

Fig. 2 Overview of expression domains of *HvAEP_FGFf* in budding *Hydra vulgaris* AEP polyps. **a** Animal carrying two late buds, *left* stage 9, *right* stage 10 ready to detach. **b**–**w** Budding stages are shown as overview (*upper row of pictures*) and close-up (*respective lower row*). Bud stages are indicated in the *upper right corner*. *tb* tentacle base (*open arrowhead*), *mg* mesogloea, the basal matrix between ecto- and endoderm is indicated to allow evaluation of ecto- and /or endodermal expression. *Scale bar* **a**–**f**, **i**, **l**–**q**=250 μm, **g**–**h**, **j**–**k**, **r**–**w**=100 μm

of FGFf-positive cells during the bud elongation phase. It has to be shown whether the differences are of functional importance as seen previously for differences in protein kinase C (PKC) expression, which correlated to a differential sensitivity to PKC stimulation (Hassel 1998).

Upregulation of FGFf expression is not correlated to morphogenesis in general

Morphogenesis in *Hydra* occurs specifically to form and maintain structures, but it also occurs during early regeneration, when the wounded tissue constricts to close the body tube. Therefore, regeneration can be used to test the hypothesis that FGFf is upregulated transcriptionally during morphogenesis in general, e.g. in formation of a constriction at the wound site.

We induced regeneration by bisection and analysed FGFf expression. At none of the regeneration sites was upregulation of FGFf transcription detectable during wound closure and in the first 4 h of regeneration (Fig. 4a–f). First signs of FGFf transcripts became detectable uniformly in head regenerating fragments from 6–8 h onwards in ecto- and endodermal cells of the apical cap (Fig. 4h, j). Between 8–10 h after bisection, commitment to head structures is fixed (MacWilliams 1983), although head structures form only 30 h later. The phase, when FGFf becomes upregulated first thus corresponds to preparative head determination. From 12-h post sectioning, additional patches of ectodermal cells appeared within the weakly expressing cap (Fig. 4l). This is astonishing, because tentacle buds develop no earlier than 36 h after bisection. In the following 10 h, no consistent expression either in a uniform cap or in a cap plus additional patches could be observed, although 10 animals per time point were analysed. At 14 h, both animals with a cap and such with patches were found; at 16 h, only the cap staining appeared and at 24 h, cap plus patchy staining were detected. The patches became stronger with time (Fig. 4n, p, r). Around 30 h after cutting, the cap staining became more intensive and the patches almost disappeared within the broad and strong

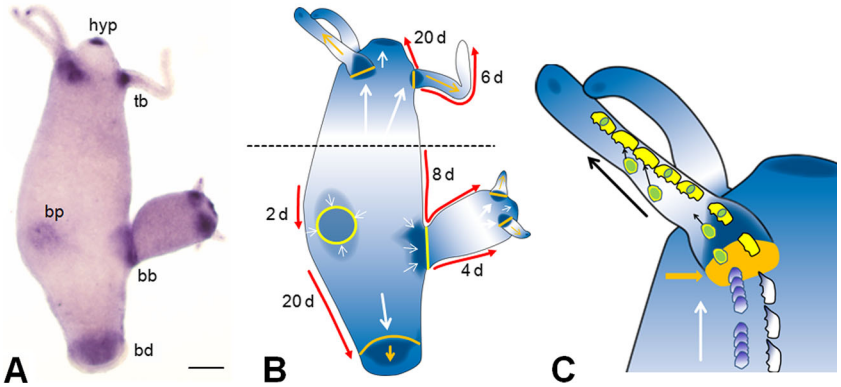

Fig. 3 Overview of expression domains of *HvAEP_FGFf* in a budding *Hydra vulgaris* Zürich polyp and model to explain FGF functions. **a** Whole *Hydra* carrying a stage 8 bud and a putatively developing early bud placode (bp). *hyp* hypostome, *tb* tentacle base, *bb* bud base, *bd* basal disc. **b** Model for the chemoattractive and differentiation-inducing effects of *FGFf* and formation of gradients. *Dotted line* region from which tissue moves either up or down the body column (Campbell 1967). *Red arrows* indicate in which direction tissue moves and how long it takes (days) to reach a certain destination. *Dark blue* are sources of *FGFf* and its gradients (*blue*), *white arrows* indicates potential attraction of cells towards termini and boundaries. The *yellow zones* at the bud base and surrounding the bud placode mark the boundary (high FGF) through which cells move to form the evaginating bud. The *orange zones and arrows* at tentacle base and basal disc indicate a potential differentiation signal. Thereafter, cells in the tentacles might respond to FGFf and move towards the tentacles tips. **c** Model for cell movement into the tentacles and differentiation signals. *Orange zone and arrow* indicate (*FGFf*) differentiation signal. Epitheliomuscular cells (*bluewhite*) become battery cells (*yellow*); nematoblasts (*roundish blue white* cell nests in the body column) become nematocytes (*green with a yellow rim*). *Black arrows* indicate directional movement of nematocytes in the tentacle. An additional signal (not FGFf) directs them into the battery cells. *Scale bar*=100 μm

ectodermal apical expression (Fig. 4t). At 36 h, hypostome and putative tentacle buds became visible as distinct patches (or rings) of strongly expressing (endo- and ectodermal) cells. Cap expression had completely disappeared (Fig. 4v). When tentacles started to sprout from 40–48 h onwards, weak endodermal tip expression persisted similar to that found in intact polyps (Fig. 4x).

In foot-regenerating fragments, the expression pattern was less complex. From 8 h onwards, the gene was found upregulated, weakly in ecto- and endodermal cells of the regenerating cap (Fig. 4i, k, m, o, q). At 30 h, when the foot structure becomes visible morphologically, ectodermal expression started to cease and a strong and uniform expression established in the endoderm (Fig. 4s). From 36 h onwards, the normal pattern of endodermal expression in the basal disc was attained (Fig. 4u, w). Although foot tissue forms about 24 h earlier than head structures in bisected polyps, upregulation is lagging for 2 h indicating that FGFf is subject to region-specific transcriptional control. The strong expression indicates the preparative and final phases of foot differentiation.

In head and foot regeneration, upregulation of the gene was clearly not associated with constriction morphogenesis per se (during early regeneration). It became detectable from preparative head determination (30 h prior to differentiation) and from preparative differentiation of foot structures until the pattern typical for the final structures had established. Therefore, FGFf is not a general control element of constriction formation. Its expression accompanies processes specific for structure formation.

A model for *FGFf* function

FGFs may act differentially at high and low concentrations to control cell migration and differentiation (McAvoy and Chamberlain 1989). Such concentration differences were recently used in a model to explain effects on tissue movement in *Drosophila* induced by low FGF concentrations and differentiation/cell adhesion, induced at high FGF concentrations (Bae et al. 2012). Transferred to *Hydra*, this model would predict that, deduced from the expression pattern of FGFf, cells move towards the terminal regions and into buds. In this case, however, things are not that simple.

In *Hydra*, constant cell proliferation in the body column ensures constant supply of tissue as well as differentiation products (nerves and nematocytes) for the terminal structures and for vegetative buds. Epithelial cells mostly move as sheets anchored in the underlying mesogloea (Aufschnaiter et al. 2011). This movement is caused by a balanced generation of cells in the gastric region and loss of cells at the extremities (Campbell 1967), but it is unclear how morphogenesis of distinct tentacles and buds is controlled. Epithelial cells are released at the base of both tentacles and buds, for a short period of time from the mesogloea to reorient and then anchor again in the newly formed mesogloea. FGFf marks both boundaries.

Interstitial cell derivatives like nematoblasts and neuron precursors (Boehm and Bosch 2012; David 2012), in contrast to epithelial cells, move actively towards tentacles, hypostome and basal disc. Nematocytes show the most sophisticated directional migration behaviour along the tentacles to finally

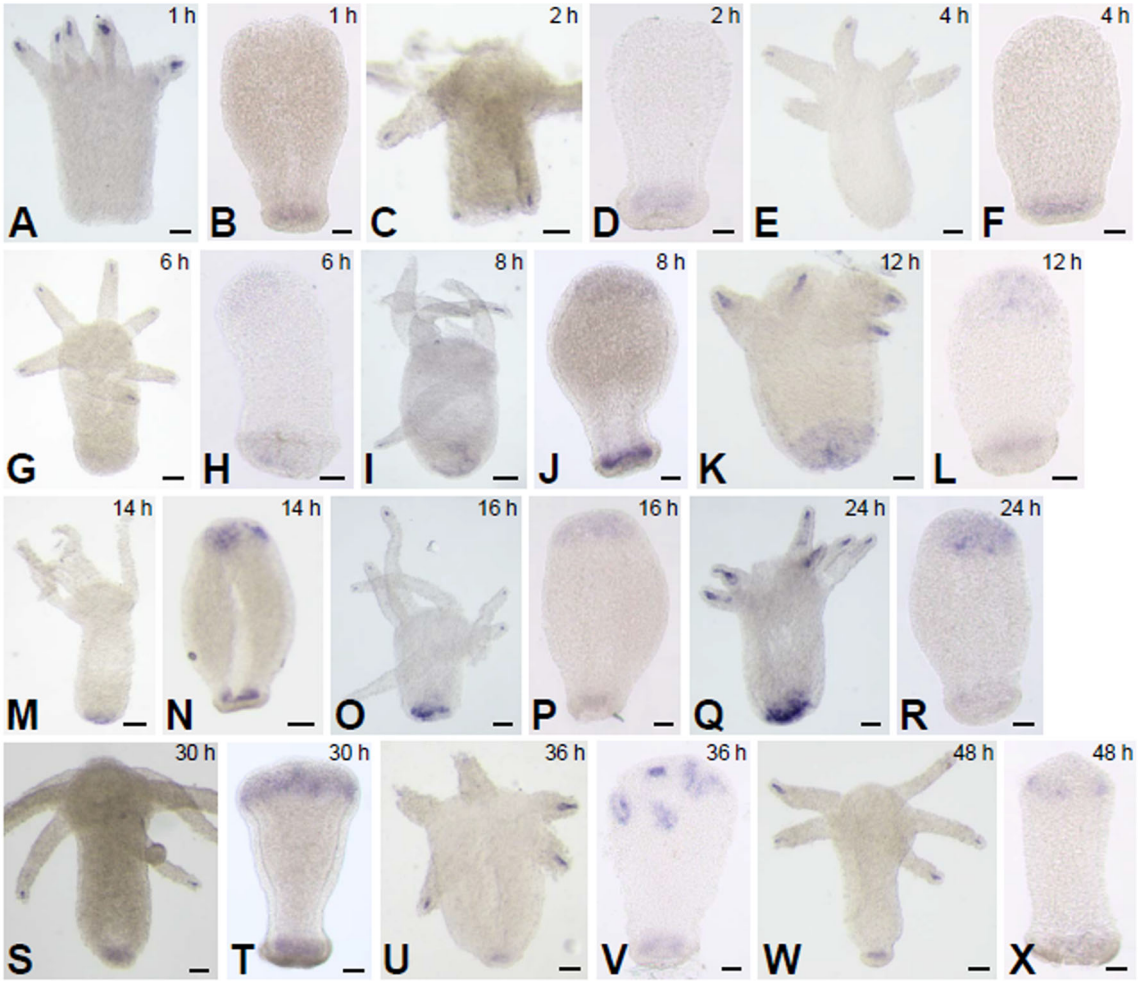

Fig. 4 Time course of FGFf expression during regeneration of head and foot structures between 1 and 48 h. Shown are regeneration of a foot (**a**, **c**, **e**, **g**, **i**, **k**, **l**, **m**, **o**, **q**, **s**, **u**, **w**) and of the head (**b**, **d**, **f**, **h**, **j**, **l**, **n**, **p**, **r**, **t**, **v**, **x**) side by side. Regeneration time points post sectioning are given in the *upper right corner*. Between 1–2 h of regeneration, the wound closes by constriction of tissue. *Scale bar*=100 μm

integrate in pouches of the battery cells in a strictly regulated spatial arrangement (Novak and Wood 1983). This clearly requires guidance cues and FGFs might be signals attracting them.

FGFs are known to control single cell movement as well as unidirectional mass tissue movement, e.g. in guidance of the mesodermal sheet between ecto- and endoderm towards its final destination in *Drosophila* (reviewed in (Kadam et al. 2012; Klingseisen et al. 2009). We recently showed that a *Hydra* FGFR is able to partially substitute for the Heartless FGFR in fly mesoderm migration (Rudolf et al. 2012). This suggests interaction with fly FGFs and conserved functions of FGF/FGFR in the animal kingdom. Deduced from its dynamic pattern during morphogenesis and in the adult polyp, *HvFGFf* appears to be an interesting candidate to act as a chemoattractant, which guides cells to certain body regions.

The N-terminal signal peptide predicted in *HvFGFf* and its assignment to the paracrine FGF8 subfamily indicates that it is likely a secreted molecule and might be diffusible as are the other members of this subfamily. Comparable to vertebrate FGF8 gradients (Bokel and Brand 2013; Scholpp and Brand 2004), *HvFGFf* might establish short and long ranging gradients along the body column depending on binding to the extracellular matrix or by differential endocytosis. In normal polyps, interstitial cells of the body column (neuroblasts or nematoblasts) might thus be attracted towards an FGF source in the basal disc (to end up as, e.g. neurons) and in the upper body column towards the FGF sources at the tentacle base and further towards the tip or between tentacles to the mouth opening to end up as neurons or nematocytes.

A unifying model for *HvFGFf* functions (Fig. 3b) is therefore based on the localized expression of *HvFGFf* which provides sources (and by diffusion generates gradients). The gradients should run from the apical and basal body column towards the middle and attract interstitial cells towards the basal disc, the hypostome and the tentacle base. Moreover, nematocytes move along the tentacle battery cells with

astonishing precision and integrate in a highly regulated pattern to refill nematocytes lost during capture of prey (Novak and Wood 1983). They might be guided by chemoattraction through the FGFf source at the tentacle tip (Fig. 3c) and directed by other signals to specifically integrate into the battery cell. As for epithelial cells of the body column, the high *FGFf* concentrations at the tentacle base might provide the signal to transdifferentiate into battery cells (Fig. 3c).

In agreement with the model, one or several FGFs at the tentacle base could instruct cells by generating multiple differentiation, guidance and sorting signals.

The above-presented simplified model could not explain the function of FGFf in the bud placode, where no particular cell differentiation or migration occurs as far as is known. The tissue here undergoes morphogenetic movement and cell shape changes allow evagination controlled by WNT signalling (Philipp et al. 2009). Yet, FGF signalling might have a complementary function in the control of cell morphogenesis and regulation of the actin cytoskeleton: when cell shape changes occur, e.g. by apical constriction of cells during morphogenesis in the zebrafish, FGFR signalling is known to target the actin cytoskeleton (Harding and Nechiporuk 2012). In *Hydra*, *FGFf* expression domains at boundaries and termini, in fact, correlate with regions of massive cell shape changes (Aufschnaiter et al. 2011; Graf and Gierer 1980). Only apical and basal constriction of cells is able to generate the cell shape changes required to form the protruding tentacles or the bud and to constrict and close the ends of the tubular body column at mouth opening, tentacle tips and basal disc.

First regeneration experiments showed that FGFf transcription is correlated to (preparative) structure determination and differentiation, but not to simple tissue constriction at the wound edges. FGFf upregulation is thus tightly coupled to structure formation and not to constriction morphogenesis in general. Future investigations on the protein level will show which functions *FGFf* fulfils at boundaries and termini.

Conclusion

Our data provide evidence that at least three of the seven FGF subfamilies were already present before the split of Cnidaria and Bilateria. *Hydra FGFf*, a growth factor belonging to the FGF8/17/18/24 subfamily, is a promising candidate molecule to either direct cell movement, to generate the signal for terminal differentiation or to control cell shape changes coupled to structure formation. Further characterization of this molecule and of its functional implications on a protein level is now required to elucidate its functions and learn more about the evolution of FGFs.

Acknowledgments We thank Heide Brandtner for the care of our *hydra* cultures and Katja Gessner for the help with EndNote. Our referees helped with their constructive comments to improve the manuscript.

References

Abascal F, Zardoya R, Posada D (2005) ProtTest: selection of best-fit models of protein evolution. Bioinforma 21:2104–2105

Affolter M, Zeller R, Caussinus E (2009) Tissue remodelling through branching morphogenesis. Nat Rev Mol Cell Biol 10:831–842. doi:10.1038/nrm2797

Aufschnaiter R et al (2011) In vivo imaging of basement membrane movement: ECM patterning shapes *Hydra* polyps. J Cell Sci 124:4027–4038. doi:10.1242/jcs.087239

Bae YK, Trisnadi N, Kadam S, Stathopoulos A (2012) The role of FGF signaling in guiding coordinate movement of cell groups: guidance cue and cell adhesion regulator? Cell Adh Migr 6:397–403. doi:10.4161/cam.21103

Bertrand S, Iwema T, Escriva H (2014) FGF signaling emerged concomitantly with the origin of Eumetazoans. Mol Biol Evol 31:310–318. doi:10.1093/molbev/mst222

Boehm AM, Bosch TC (2012) Migration of multipotent interstitial stem cells in *Hydra* zoology. Jena 115:275–282. doi:10.1016/j.zool.2012.03.004

Bokel C, Brand M (2013) Generation and interpretation of FGF morphogen gradients in vertebrates. Curr Opin Genet Dev 23:415–422. doi:10.1016/j.gde.2013.03.002

Campbell RD (1967) Tissue dynamics of steady state growth in *Hydra littoralis*. II Patterns of tissue movement. J Morphol 121:19–28. doi:10.1002/jmor.1051210103

David CN (2012) Interstitial stem cells in *Hydra*: multipotency and decision-making. Int J Dev Biol in press

Dehal P, Boore JL (2005) Two rounds of whole genome duplication in the ancestral vertebrate. PLoS Biol 3:e314. doi:10.1371/journal.pbio.0030314

Eddy SR (2008) A probabilistic model of local sequence alignment that simplifies statistical significance estimation. PLoS Comput Biol 4:e1000069

Gouy M, Guindon S, Gascuel O (2010) SeaView version 4: a multiplatform graphical user interface for sequence alignment and phylogenetic tree building. Mol Biol Evol 27:221–224

Graf L, Gierer A (1980) Size, shape and orientation of cells in budding hydra and regulation of regeneration in cell aggregates Wilhelm Rouxs. Arch of Dev Biol 188:141–151

Harding MJ, Nechiporuk AV (2012) Fgfr-Ras-MAPK signaling is required for apical constriction via apical positioning of Rho-associated kinase during mechanosensory organ formation. Development 139:3130–3135. doi:10.1242/dev.082271

Hassel M (1998) Upregulation of a *Hydra vulgaris* cPKC gene is tightly coupled to the differentiation of head structures. Dev Genes Evol 207:489–501

Hemmrich G, Bosch TC (2008) Compagen, a comparative genomics platform for early branching metazoan animals, reveals early origins of genes regulating stem-cell differentiation. Bioessays 30:1010–1018

Hemmrich G, Anokhin B, Zacharias H, Bosch TC (2007) Molecular phylogenetics in *Hydra*, a classical model in evolutionary developmental biology. Mol Phylogenet Evol 44:281–290. doi:10.1016/j.ympev.2006.10.031

Huang P, Stern MJ (2005) FGF signaling in flies and worms: more and more relevant to vertebrate biology. Cytokine Growth Factor Rev 16:151–158. doi:10.1016/j.cytogfr.2005.03.002

Itoh N, Ornitz DM (2011) Fibroblast growth factors: from molecular evolution to roles in development, metabolism and disease. J Biochem 149:121–130

Jovelin R et al (2010) Evolution of developmental regulation in the vertebrate FgfD subfamily. J Exp Zool B Mol Dev Evol 314:33–56. doi:10.1002/jez.b.21307

Kadam S, McMahon A, Tzou P, Stathopoulos A (2009) FGF ligands in *Drosophila* have distinct activities required to support cell migration and differentiation. Development 136:739–747. doi:10.1242/dev.027904

Kadam S, Ghosh S, Stathopoulos A (2012) Synchronous and symmetric migration of *Drosophila* caudal visceral mesoderm cells requires dual input by two FGF ligands. Development. doi:10.1242/dev.068791

Klingseisen A, Clark IB, Gryzik T, Muller HA (2009) Differential and overlapping functions of two closely related *Drosophila* FGF8-like growth factors in mesoderm development. Development 136:2393–2402

Krishnapati LS, Ghaskadbi S (2013) Identification and characterization of VEGF and FGF from *Hydra*. Int J Dev Biol 57:897–906. doi:10.1387/ijdb.130077sg

MacWilliams HK (1983) Hydra transplantation phenomena and the mechanism of *Hydra* head regeneration. II. Properties of the head activation. Dev Biol 96:239–257

Matus DQ, Thomsen GH, Martindale MQ (2007) FGF signaling in gastrulation and neural development in *Nematostella vectensis*, an anthozoan cnidarian. Dev Genes Evol 217:137–148

McAvoy JW, Chamberlain CG (1989) Fibroblast growth factor (FGF) induces different responses in lens epithelial cells depending on its concentration. Development 107:221–228

Muha V, Muller HA (2013) Functions and mechanisms of fibroblast growth factor (FGF) signalling in *Drosophila melanogaster*. Int J Mol Sci 14:5920–5937. doi:10.3390/ijms14035920

Neron B et al (2009) Mobyle: a new full web bioinformatics framework. Bioinformatics 25:3005–3011

Novak PL, Wood RL (1983) Development of the nematocyte junctional complex in hydra tentacles in relation to cellular recognition and positioning. J Ultrastruct Res 83:111–121

Otto J, Campbell R (1977) Budding in *Hydra attenuata*: bud stages and fate map. J Exp Zool 200:417–428. doi:10.1002/jez.1402000311

Oulion S, Bertrand S, Escriva H (2012) Evolution of the FGF Gene Family International Journal of Evolutionary Biology 2012: 298147 doi:10.1155/2012/298147

Philipp I et al (2009) Wnt/beta-Catenin and noncanonical Wnt signaling interact in tissue evagination in the simple eumetazoan. Hydra Proc Nat Acad Sci USA 106:4290–4295. doi:10.1073/pnas.0812847106

Rebscher N, Deichmann C, Sudhop S, Fritzenwanker J, Green S, Hassel M (2009) Conserved intron positions in FGFR genes reflect the modular structure of FGFR and reveal stepwise addition of domains to an already complex ancestral FGFR. Dev Genes Evol 219:455–468. doi:10.1007/s00427-009-0309-5

Rentzsch F, Fritzenwanker JH, Scholz CB, Technau U (2008) FGF signalling controls formation of the apical sensory organ in the cnidarian *Nematostella vectensis*. Development 135:1761–1769. doi:10.1242/dev.020784

Ronquist F et al. (2012) MrBayes 3.2: efficient Bayesian phylogenetic inference and model choice across a large model space Syst Biol 61: 539-542

Rudolf A et al. (2012) The Hydra FGFR, Kringelchen, partially replaces the *Drosophila* heartless FGFR Dev Genes Evol doi:10.1007/s00427-012-0424-6

Satou Y, Imai KS, Satoh N (2002) Fgf genes in the basal chordate *Ciona intestinalis*. Dev Genes Evol 212:432–438. doi:10.1007/s00427-002-0266-8

Scholpp S, Brand M (2004) Endocytosis controls spreading and effective signaling range of FGF8 protein. Curr Biol 14:1834–1841. doi:10.1016/j.cub.2004.09.084

Sudhop S, Coulier F, Bieller A, Vogt A, Hotz T, Hassel M (2004) Signalling by the FGFR-like tyrosine kinase, Kringelchen, is essential for bud detachment in *Hydra vulgaris*. Development 131:4001–4011. doi:10.1242/dev.01267

Wenger Y, Galliot B (2013) RNAseq versus genome-predicted transcriptomes: a large population of novel transcripts identified in an Illumina-454 *Hydra* transcriptome. BMC Genomics 14:204